

# In-band Spectra and Filter Shape Monitoring Using High-resolution Swept Coherent Detection

Xiangqing Tian<sup>1</sup>, Yikai Su<sup>1</sup>, Peigang Hu<sup>1</sup>, Hao He<sup>1</sup>, Lufeng Leng<sup>2</sup>, Weisheng Hu<sup>1</sup>,  
Haigen Shen<sup>1</sup>, Lilin Yi<sup>1</sup>, Li Zhan<sup>1</sup>

<sup>1</sup>State Key Lab of Advanced Optical Communication Systems and Networks, Shanghai Jiao Tong University  
Shanghai 200240, China, Email: tianxq@sjtu.edu.cn

<sup>2</sup>New York City College of Technology, City University of New York, 300 Jay Street, Brooklyn,  
NY 11201, USA

## ABSTRACT

In this paper, a novel in-band optical spectra and filter shape monitoring technique is experimentally demonstrated. Based on swept coherent detection, the proposed technique simultaneously measures the signal and ASE spectra by adjusting the polarization states of the signal and local oscillator. In our experiment, a high resolution of 0.002 nm is achieved.

**Keywords:** Coherent detection, optical performance monitoring, optical signal-to-noise-ratio (OSNR), spectral analysis.

## 1. INTRODUCTION

In future reconfigurable wavelength division multiplexing (WDM) networks, each data channel may go through a path employing multiple wavelength multiplexers/demultiplexers of different types. The in-band amplified spontaneous emission (ASE) noise from the amplifiers accumulates while the out-of-band noise is cut down by the filters. Conventional optical spectrum analyzers (OSAs) cannot distinguish the in-band ASE noise from the signal, although it is a major factor that determines the transmission performance. In addition, the increasing bandwidth demands in optical networks have driven network designs towards more closely spaced wavelength channels as well as higher transmission bit rates. In some cases, channel spacing has migrated to 12.5 GHz or even 6.25 GHz [1]. However, the resolution bandwidths (RBs) of most OSAs are not sufficient to reveal the signal spectra with such channel spacings. All these have imposed technical challenges to conventional grating based OSAs. Swept coherent detection [2-4] is a promising technique which shows high resolution for optical spectrum measurement. However, previous reports have mainly focused on dynamic range in the measurement, while the important details such as the in-band ASE spectrum and the shape of the cascaded filters cannot be obtained.

In this paper, a novel in-band optical spectra and filter shape monitoring technique has been proposed. A nice feature of our scheme is that it provides an effective approach to simultaneously monitoring in-band ASE and optical signal spectra in WDM networks. The proposed scheme is based on swept coherent detection, which converts the optical signal down to RF domain. Owing to the strong processing capability and matured technique of RF electronics, we can measure the in-band ASE and optical signal in a very precise manner. The signal and the noise are detected separately by properly adjusting the polarization states of the signal and the wavelength-tunable local oscillator (LO). As shown in subsequent section, when the signal and the LO are aligned to have the same polarization states, the signal spectrum is obtained. While when they are orthogonally polarized, the in-band ASE spectrum can be measured. In our experiment, a high resolution of 0.002 nm is shown, which is far beyond the RBs of most grating based OSAs. The only limitation of resolution in our experiment is the tuning step of the LO or the data processing capability.

## 2. OPERATION PRINCIPLE

Fig.1 shows the principle of our proposed scheme. The swept coherent detector part contains a wavelength tunable laser as the local oscillator, a balanced receiver and a RF spectrum analyzer. The balanced receiver is used

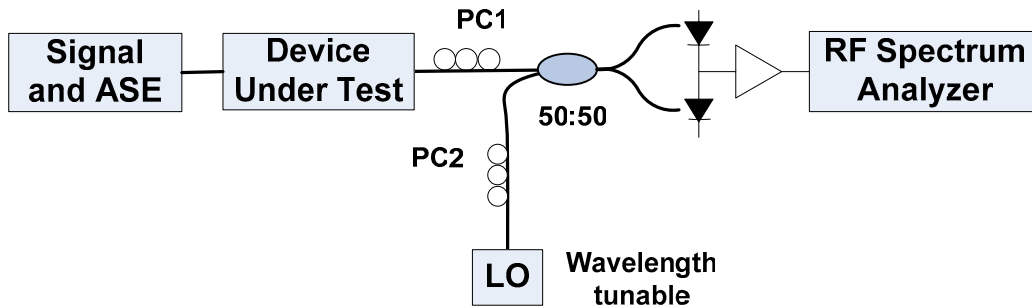


Fig.1 Schematic of swept coherent detection

to eliminate the baseband signal after heterodyne detection. The filtered ASE noise at a specific frequency can be written as:

$$E_{ASE}(t) = \sum_i |A_i| \cdot \exp[j2\pi f_i t + j\varphi_i(t)] \vec{p}_{ASE,i} \quad (1)$$

where  $A_i$ ,  $\varphi_i(t)$  and  $\vec{p}_{ASE,i}$  are random variables to denote the amplitude, phase, and polarization, respectively, of the ASE component at frequency  $f_i$ .

Similarly, the fields of optical signal and LO are:

$$E_S(t) = \sum_k |A_{S,k}| \cdot \exp[j2\pi f_{S,k} t + j\varphi_{S,k}(t)] \vec{p}_S \quad (2)$$

$$E_{LO}(t) = |A_{LO}| \cdot \exp[j2\pi f_{LO} t + j\varphi_{LO}(t)] \vec{p}_{LO} \quad (3)$$

where  $\vec{p}_S$  and  $\vec{p}_{LO}$  in Eq.(2) and (3) are the polarization states of the signal and LO. At the 50:50 coupler, the output optical field are:

$$\begin{pmatrix} E_1(t) \\ E_2(t) \end{pmatrix} = \begin{pmatrix} \sqrt{\rho} & j\sqrt{1-\rho} \\ j\sqrt{1-\rho} & \sqrt{\rho} \end{pmatrix} \cdot \begin{pmatrix} E_S(t) + E_{ASE}(t) \\ E_{LO}(t) \end{pmatrix} \quad (4)$$

where  $\rho$  is the splitting ratio. For the 50:50 coupler,  $\rho=0.5$ . After the balanced receiver, the electrical output can be derived as:

$$\begin{aligned} P_E(t) &\propto |E_1(t)|^2 - |E_2(t)|^2 \\ &\propto |E_S(t) + E_{ASE}(t) + jE_{LO}(t)|^2 - |E_S(t) + E_{ASE}(t) - jE_{LO}(t)|^2 \\ &\propto |A_{LO}| \cdot \sum_k |A_{S,k}| \sin\{2\pi(f_{LO} - f_{S,k})t + j[\varphi_{LO}(t) - \varphi_{S,k}(t)]\} \vec{p}_{LO} \cdot \vec{p}_S \\ &\quad + |A_{LO}| \cdot \sum_i |A_i| \sin\{2\pi(f_{LO} - f_i)t + j[\varphi_{LO}(t) - \varphi_i(t)]\} \vec{p}_{LO} \cdot \vec{p}_{ASE,i} \end{aligned} \quad (5)$$

As Eq.(5) shows, the direct-detected parts of the signal and LO, such as  $|E_S(t)|^2$  and  $|E_{LO}(t)|^2$ , have been eliminated by the balanced nature of the receiver, and only the beating terms between signal, LO and ASE are left. At the spectrum analyzer, the electrical power is given by :

$$\begin{aligned} \langle P_E(t) \rangle &\propto |A_{LO}|^2 \cdot \left( \sum_k |A_k| |\vec{p}_{LO} \cdot \vec{p}_S| \right)^2 + |A_{LO}|^2 \cdot \left\langle \left( \sum_i |A_i| |\vec{p}_{LO} \cdot \vec{p}_{ASE,i}| \right)^2 \right\rangle \\ &\propto |A_{LO}|^2 P_S |\vec{p}_{LO} \cdot \vec{p}_S| + \frac{1}{2} |A_{LO}|^2 P_{ASE} \end{aligned} \quad (6)$$

where  $\langle \cdot \rangle$  denotes time average,  $P_S$ ,  $P_{ASE}$  are the optical power of the signal and ASE. The first term in (6) is the signal-LO beating component, while the second one stands for the ASE-LO beating term. The factor of one half in

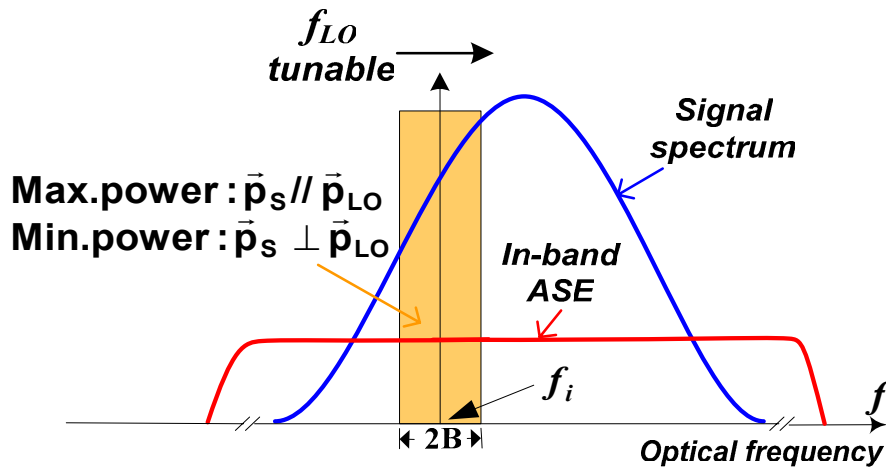


Fig.2 Operation principle of in-band high-resolution swept coherent detection scheme

the second term is due to  $\vec{p}_{ASE,i}$  being a random variable [5, 6]. It can be seen that, when  $\vec{p}_S // \vec{p}_{LO}$ ,  $\vec{p}_S \cdot \vec{p}_{LO} = 1$ , there is a maximal output at the RF spectrum analyzer as Eq.(6) shows, and this output is a direct indicator of the optical signal power at a specific frequency. While when  $\vec{p}_S \perp \vec{p}_{LO}$ ,  $\vec{p}_S \cdot \vec{p}_{LO} = 0$ , the receiver outputs a minimal signal, as in this case only the beat product between ASE noise and LO is produced. The signal is "blocked" due to the orthogonal polarization of the signal and the LO. By continuously tuning the wavelength of the LO, the receiver scans over the whole wavelength range of the optical signal, and provides a highly resolved optical spectrum. At the RF spectrum analyzer, only the frequency components that satisfy  $|f_{LO} - f_i| < B$  will be monitored, where  $B$  is the monitoring bandwidth as shown in Fig.2, and it is also the resolution bandwidth. The detected electrical power at frequency  $f_{LO}$  is linearly related to the optical power at frequency  $f_i$ . In the experiment, the limitation in resolution is the tuning step of the LO or the data processing capability. In our experiment, to achieve high resolution while keeping a reasonable number of sampling points, we chose the sweeping step of the LO to be 0.002 nm, and consequently the monitoring bandwidth is set to be  $B=130$  MHz.

### 3. EXPERIMENTAL SETUP AND RESULTS

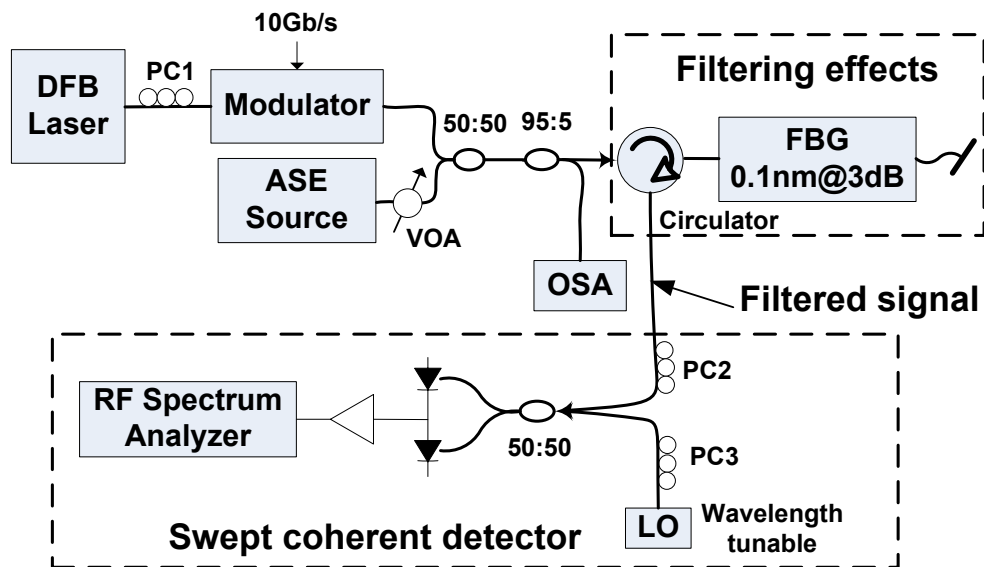
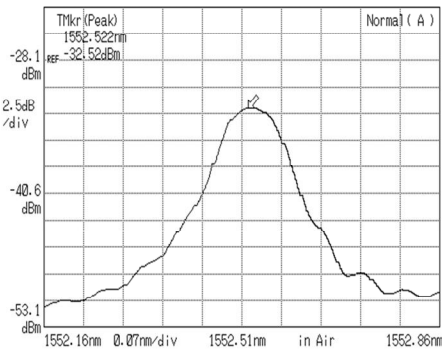
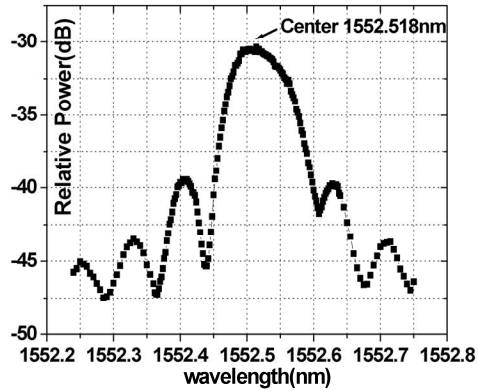


Fig.3 experimental setup for in-band spectra monitoring based on swept coherent detection. PC: Polarization Controller, FBG: Fiber Bragg Grating

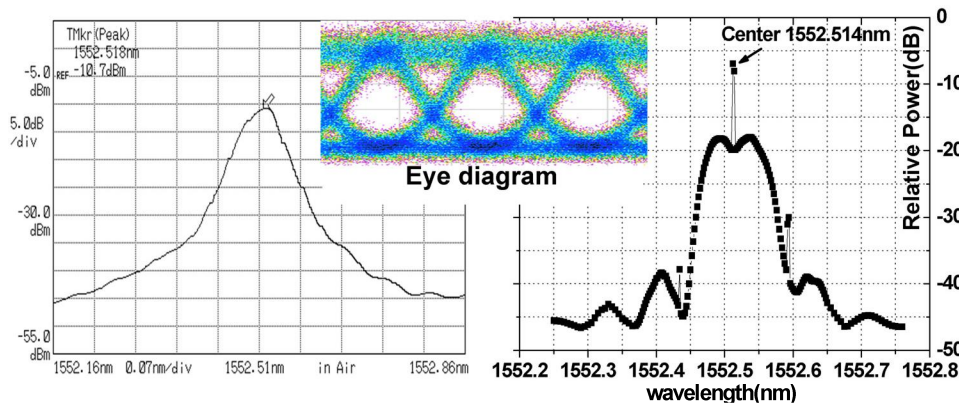


(a) Measured by OSA



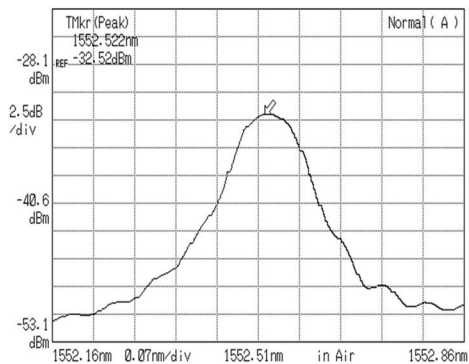
(b) Measured by our scheme

Fig.4 In-band ASE spectra measured by OSA and swept coherent detection

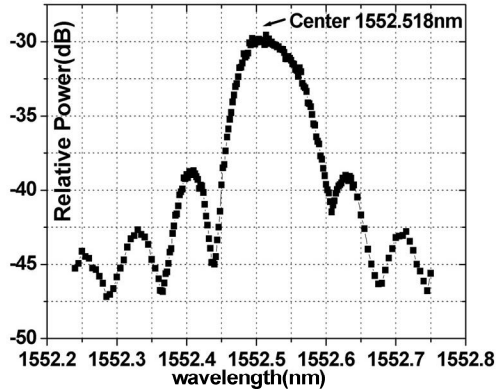


(a) Signal spectrum

(c) Signal spectrum



(b) In-band ASE spectrum



(d) In-band ASE spectrum

Fig.5 Optical spectra of the signal and the in-band ASE. The inset is the eye diagram of the filtered 10-Gb/s NRZ signal at an OSNR of 21.3 dB. (a) and (b) are measured by the OSA set at 0.07 nm RB. (c) and (d) are measured by the swept coherent detector.

The schematic of experimental setup is shown in Fig.3. To test the performance of our proposed scheme when there is modulated signal, we modulate the distributed-feedback (DFB) laser by 10-Gbit/s non-return-to-zero (NRZ) signal (pattern length:  $2^{31}-1$ ) using a LiNbO<sub>3</sub> modulator. The ASE passes through a variable attenuator and is then combined by a coupler with the modulated signal. One part of the multiplexed signal is sent to the OSA, while the other part is sent to the fiber Bragg grating (FBG), which is used to mimic the filtering effect. The FBG is centered at 1552.52 nm, and its 3 dB bandwidth is  $\sim 0.1$  nm. The swept coherent detection part contains a wavelength tunable laser as the local oscillator, a balanced receiver pair and a RF spectrum analyzer.

We first measured the in-band ASE by switching off the DFB laser. Here we assume that the ASE noise has flat power distribution over a wide range of wavelength, so the measured in-band ASE is also the filter shape. The results are shown in Fig.4. We then turn on the DFB laser, and measure in-band optical spectra by adjusting the polarization states of the signal and LO. The results are shown in Fig.5, where the distortion in the eye diagrams is due to tight filtering. It is clearly shown that the proposed method has much higher resolution than the OSA.

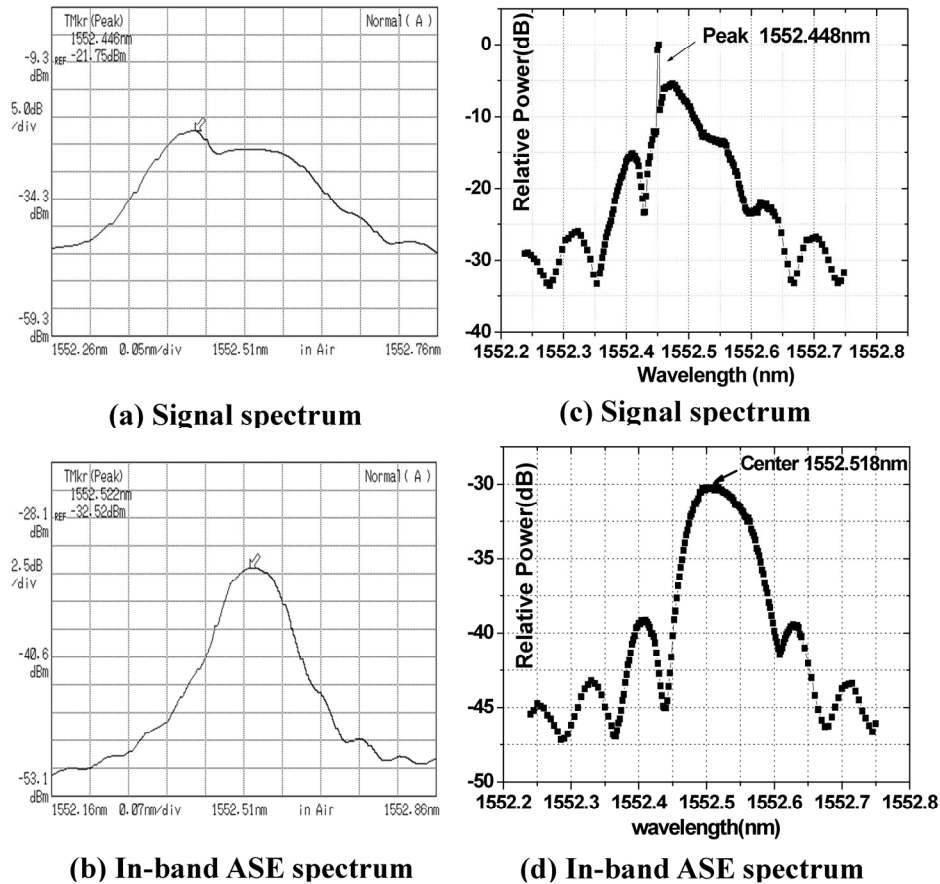


Fig.6 Optical spectra of the signal and the in-band ASE with 0.07 nm misalignment (a) and (b) are measured by the OSA set at 0.07nm RB. (c) and (d) are measured by the swept coherent detector.

Fig.4(b) is the in-band ASE noise measured by swept coherent detector. The sideband peaks and dips of the FBG filter are clearly shown by the in-band ASE. However, with the conventional OSA, the details of the FBG passband cannot be seen due to the limited resolution of the OSA. Also, we observe that there is little difference between Fig.4(b) and Fig.5(d), showing that the modulated signal has been properly “blocked” by polarization, and that the in-band ASE reveals the filter shape even when the modulated signal is present. Fig.5(c) shows very fine structures of the NRZ signal, the sideband tones are clearly visible using our scheme.

Our swept coherent detector can also be used to precisely measure the misalignment between signal peaks and middle of filters. Fig.6 shows the measured results when we misaligned the central of the modulated signal by about 0.07 nm. The measured misalignment is 0.07 nm and 0.076 nm respectively by swept coherent detection and OSA. Again it shows the good accuracy of our proposed scheme. It should be pointed out that when we measure the misalignment using OSA, we must turn off the DFB laser to obtain the filter shape, which is impractical in real system. While if our swept coherent detector is used, there is no need to turn off the transmitter, and it can achieve in-line operation. Again, we can see that there are little difference between the in-band ASE shapes, as shown in Fig.5(d) and Fig.6(d), although the misalignment is considered, showing well “blocking” of the signal by the orthogonal polarization states between the signal and LO.

#### 4. CONCLUSIONS

In this paper, a simple, low-cost in-band optical spectra monitoring technique is proposed. Using polarization controlled swept coherent detection, the proposed scheme realizes simultaneous in-band ASE and signal spectra monitoring. Owing to the strong processing capability and matured technique of RF electronics, it eliminates the need for any high speed components, and is independent of data rate. In our experiment, measurements of in-band ASE spectrum and misalignment between central of signal and filter are demonstrated. A very high resolution of 0.002nm is achieved. This provides an effective approach to realizing in-band monitoring of signal, noise and filter shape in WDM networks.

#### ACKNOWLEDGEMENT

The authors acknowledge that the funding for this project was provided by the NSFC under the grants 60407008/90304002, Shanghai Optical Science and Technology grant 04dz05103, and Shanghai Rising Star program 04QMX1413.

#### REFERENCES

1. Takara, H.; Ohara, T.; Yamamoto, T.; Masuda, H.; Abe, M.; Takahashi, H.; Morioka, T, “Field demonstration of over 1000-channel DWDM transmission with supercontinuum multi-carrier source”, *Electronics Letters*, vol.41, pp.270-271, Mar 2005,

2. D. M. Baney,, B. Szafraniec,, and A. Motamedi., “Coherent Optical Spectrum Analyzer”, *IEEE Photon. Technol. Lett.*, vol. 14, pp.355-357, Mar. 2002.
3. B. Szafraniec, A. Motamedi, D. M. Baney, “Polarization-diverse coherent optical spectrum analyzer with swept local oscillator”, in *Tech. Dig. OFC 2002*, ThGG5.
4. S. Yoshida, Y. Tada, and K. Nosu, “High resolution optical spectrum analysis by coherent detection with multi-electrode DBR-LD’s as local oscillators,” in *Conf. Proc. IMTC/94. IEEE Instrumentation Measurement Technology Conf.*, vol. 1, 1994, pp. 230–233.
5. J. H. Lee, D. K. Jung, C. H. Kim, and Y. C. Chung, “OSNR monitoring technique using polarization-nulling method,” *IEEE Photon. Technol. Lett.*, vol. 13, pp.88-90, Jan. 2001.
6. M. H. Cheung, L. K. Chen, and C. K. Chan, “PMD-insensitive OSNR monitoring based on polarization-nulling with off-center narrow-band filtering,” *IEEE Photon. Technol. Lett.*, vol. 16, pp.2562-2564, Nov. 2004.